A Multi-Sensor Fault Diagnosis Method for Aero-Engine Bearings Based on Complex-Valued Convolution and Dual Attention Mechanism

Shuquan Xiao[1], Xueyi Li[2,3], Tianyang Wang[3], and Fulei Chu[4]

[1,2]*College of Mechanical and Electrical Engineering, Northeast Forestry University, Harbin 150040, China*
xiaoshuquan@nefu.edu.cn
lixueyi@nefu.edu.cn

[3,4]*Department of Mechanical Engineering, Tsinghua University, Beijing 100084, China*
wty19850925@tsinghua.edu.cn
chufl@mail.tsinghua.edu.cn

ABSTRACT

Aero engines are widely used in modern aviation due to their high thrust-to-weight ratio, high efficiency, and high reliability, placing greater demands on the operational safety of key components such as bearings. Traditional bearing fault diagnosis methods typically rely on vibration signals collected by a single sensor, which makes it difficult to handle challenges such as incomplete information and noise interference in industrial settings. The paper proposes an intelligent fault diagnosis model called the Time-Frequency Attention Network, which is based on a time-frequency-aware convolutional layer and a fused attention mechanism. The goal is to fully exploit the time-frequency feature information from multi-sensor signals. First, a time-frequency-aware convolutional layer is designed using a kernel function constrained by the Short-Time Fourier Transform, leveraging a complex-valued convolution structure to effectively extract non-stationary features and local instantaneous frequency variations. Subsequently, a fused attention module is constructed, introducing a dual-attention mechanism in both channel and spatial dimensions to adaptively adjust the response intensity and frequency-domain focus areas of different sensor signals. The proposed network is experimentally validated on the Harbin Institute of Technology bearing dataset, achieving an accuracy of 99.54%. The results demonstrate that the proposed method outperforms existing benchmark models in terms of fault recognition accuracy and robustness, showcasing excellent diagnostic performance and generalization ability.

Keywords: Bearing fault diagnosis; Attention mechanism; Multi-sensor; Complex-valued convolution.

1. INTRODUCTION

Aero engines are widely used in modern aviation due to their high thrust-to-weight ratio, high efficiency, and high reliability. As their performance continues to improve, there is an increasing demand for advanced intelligent maintenance technologies, particularly in ensuring the operational reliability of key components such as bearings, gears, and shafts (Dai, Liang, Li, Wu & Wang, 2025). If faults are not identified accurately and in a timely manner during operation, they can easily lead to systemic failures, resulting in significant economic losses and even safety accidents. Therefore, fault diagnosis of bearings is a crucial measure to ensure their operational safety and reliability.

Current fault diagnosis methods primarily rely on vibration signals collected by a single accelerometer. For example, a sparsity-controllable sparse morphological decomposition method has been proposed to efficiently identify prominent shift-invariant components containing impulsive features, aiming to enhance the accuracy and robustness of fault diagnosis for high-speed bearings (Kim & Lee, 2025). To further improve fault diagnosis performance, another novel approach combines multi-kernel Maximum Mean Discrepancy and multi-kernel Conditional Maximum Mean Discrepancy to propose a new joint distribution discrepancy measure. By enhancing domain confusion effects, this method effectively captures fault features even when data distributions are imbalanced or exhibit significant variation (Li, Chen & Li, 2025). To address issues such as low diagnostic accuracy and poor robustness, a multi-branch feature fusion module is constructed to capture multi-scale correlation information within the signals, enabling adaptive learning of fault features at different levels (Liu, Chen, Li, Zhou & Wu, 2025). The methods mentioned in the above literature all rely on single-sensor data for fault diagnosis. However, in real industrial environments, complex bearing component systems may face challenges such as insufficient

fault feature information and difficulty in extracting critical features when using fault diagnosis methods based solely on a single sensor.

In order to address the instability and information incompleteness of single sensor data fault diagnosis in practical industrial environments, researchers have gradually adopted multi-sensor data input to obtain comprehensive information about equipment operation from different perspectives, enabling a more comprehensive fault feature representation. By analyzing the correlation between different sensors and samples, multi-layer graph data is constructed to achieve multi-sensor data level fusion (Xiao, Li & He, 2025). For the early weak fault diagnosis of bearings, principal component analysis is used to combine vibration signals from multiple sensors in both horizontal and vertical directions, making full use of the feature information from multi-sensor signals (Xu, Chen & Xu, 2025). A global feature perception mechanism is constructed by integrating a multi-sensor sparse Transformer and a hierarchical architecture, fully exploiting the global features specific to each sensor as well as the cross-sensor global features between multiple sensors (Yang, Li, Xue & He, 2025). In summary, bearing fault diagnosis methods still have vast potential for improvement in processing signal sequences and exploring their internal correlations. From initially relying on signals from a single sensor to gradually integrating multi-sensor data, bearing fault diagnosis strategies are continuously evolving towards multi-source, multi-dimensional, and multi-scale information fusion. However, challenges remain in effectively coordinating high-dimensional heterogeneous data, suppressing redundant information, and modeling the relationships between deep features. For example, when applying convolutional neural networks for multi-source information fault diagnosis, there is a lack of specificity, making it difficult to effectively capture the relationships between different information sources. Additionally, the limited local receptive field of convolutional kernels requires stacking a large number of convolutional layers to obtain global information. Therefore, in order to efficiently extract fault-related time-frequency information from raw vibration signals and capture long-range dependencies, this paper proposes a time-frequency attention network (TFANet) based on STFT transformation. The proposed method was validated on the Harbin Institute of Technology bearing dataset, and by comparing it with benchmark models and other methods, the results demonstrate that the proposed method has superior diagnostic performance. The contributions of this study can be summarized as follows:

1. In response to the non-stationary and time-varying nature of bearing fault signals, this paper proposes a time-frequency perception convolutional layer based on the STFT kernel function, which more accurately captures the non-stationary patterns of fault features and local instantaneous frequency variations.

2. A new feature fusion module is designed, introducing a dual attention path during the convolution process. This module adaptively adjusts the response strength and time-domain weight distribution of multi-channel bearing sensor signals, effectively highlighting the diagnostic information in key frequency regions.

2. METHODOLOGY

The proposed TFANet network is primarily composed of the time-frequency perception convolutional layer and the feature fusion module. This section will first introduce the design and mechanism of the time-frequency perception convolutional layer, followed by a detailed explanation of the implementation and role of the feature fusion module.

2.1. Time-Frequency Aware Convolutional Layer

Traditional convolutional layers often struggle to effectively extract key time-frequency features when processing vibration signals. Additionally, the single STFT method lacks the ability to adaptively extract information based on the specific characteristics of the fault dataset. In contrast, neural networks have the ability to automatically learn high-dimensional features from fault samples. Based on this, this paper proposes a time-frequency-aware convolutional layer, which aims to integrate the advantages of traditional time-frequency analysis with deep learning to more effectively extract time-frequency information from signals. This convolutional layer uses complex convolutional kernels as the core structure, with the real and imaginary parts designed as two parallel convolutional channels. By using dual-channel feature learning, it enhances the richness of feature representation. As shown in Figure 1, the time-frequency-aware convolutional layer introduces the STFT method to calculate the magnitude of the real and imaginary part features, thereby generating a time-frequency feature map, which serves as the final output of the convolutional layer.

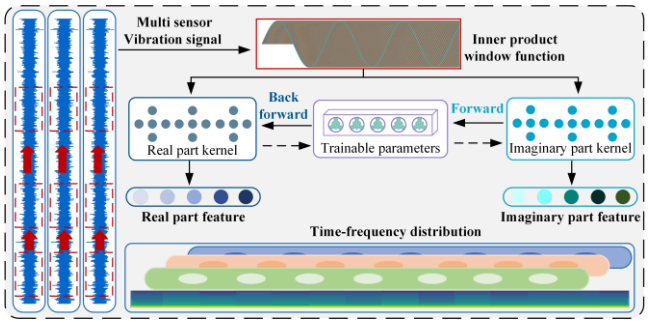

Figure 1. Time-Frequency Aware Convolutional Layer

The process is performed independently for each input channel, effectively preserving the fine-grained time-frequency structure of the original signal. The core idea of this design is to construct convolutional weights in complex form, allowing the network to simultaneously capture both the amplitude and phase variations of the signal during

feature extraction, thereby enhancing its ability to model non-stationary features. The initial convolutional kernel weights are still randomly initialized, but they are modulated and constrained by the STFT kernel function in subsequent calculations. The mathematical expression is as follows:

$$\begin{cases} \psi_\theta \in C, \quad \psi_{\theta,r}, \psi_{\theta,i} \in R \\ \psi_{\theta,r} = r(\psi_\theta) \\ \psi_{\theta,i} = i(\psi_\theta) \end{cases} \tag{1}$$

Where, ψ_θ represents the kernel function, $\psi_{\theta,r}$ and $\psi_{\theta.i}$ correspond to the real part kernel and imaginary part kernel, respectively. $r(\cdot)$ and $i(\cdot)$ are operators for the real and imaginary parts of the complex-valued function, respectively. θ represents the trainable parameters of the convolutional kernel function, which are updated during the backpropagation process.

To further clarify the modulation mechanism of the STFT kernel on the convolution kernel weights, let the input signal be $x(t)$, and its short-time Fourier transform can be expressed as:

$$X(t,f) = \int x(\tau) w(t-\tau) e^{-j2\pi f\tau} d\tau \tag{2}$$

Where, $w(\cdot)$ denotes the window function. In the time–frequency aware convolutional layer, the complex-valued convolution kernel ψ_θ can be regarded as a combination of the STFT kernel function and trainable weights, that is:

$$\psi_\theta(t,f) = \underbrace{W_\theta(t,f)}_{\text{rainable weight}} \cdot \underbrace{e^{-j2\pi ft}}_{\text{STFT modulation}} \tag{3}$$

The phase component of the convolution kernel is modulated by the STFT kernel, while its amplitude is controlled by the trainable parameters w_θ. This structure enables the network to adaptively adjust the filter's amplitude response during training, while maintaining time–frequency consistency constraints along the frequency dimension.

In the forward propagation, the complex convolution of the input signal can be expressed as:

$$y = x * \psi_\theta = (x_r + jx_i) * (\psi_{r,\theta} + j\psi_{i,\theta}) \tag{4}$$

By expanding the equation, we obtain:

$$\begin{cases} y_r = x_r * \psi_{r,\theta} - x_i * \psi_{i,\theta} \\ y_i = x_r * \psi_{i,\theta} - x_i * \psi_{r,\theta} \end{cases} \tag{5}$$

Where, y_r and y_i represent the real and imaginary parts of the output features, respectively. This structure enables the interactive fusion of real and imaginary feature components: the real part mainly reflects energy and amplitude variations, while the imaginary part carries information about phase and frequency shifts. Through joint training, the network can automatically balance the contributions of both components at the feature level, thereby enhancing its capability to model non-stationary time–frequency characteristics.

During the backpropagation process, the time-frequency-aware convolutional layer computes the gradient of the trainable parameters, and the trainable parameters are updated at each training step. The expression for this update is as follows:

$$\begin{cases} \delta_\theta = \dfrac{\partial L}{\partial H}\left(\dfrac{\partial H}{\partial \psi_{p,r}}\dfrac{\partial \psi_{p,r}}{\partial \theta} + \dfrac{\partial H}{\partial \psi_{p,i}}\dfrac{\partial \psi_{p,i}}{\partial \theta}\right) \\ \theta \leftarrow \text{optimizer}\left(\theta, \delta_\theta, \eta\right) \end{cases} \tag{6}$$

Where, θ represents the trainable parameters, δ_θ refers to the algorithm's gradient, ∂ indicates the partial derivative, L represents the classification loss, and H is the output of the time-frequency-aware convolutional layer. η is the learning rate of the optimizer.

2.2. Attention Module Integration

In the process of multi-sensor fault feature fusion, it is essential to selectively emphasize information channels and highlight important local detail features. It is recommended to redesign parts involving skip connections to facilitate the complementary interaction and effective fusion between high-dimensional and low-dimensional features. Inspired by this idea, this paper introduces a spatial-channel attention module for cross-combination, named the fusion attention module, as shown in Figure 2.

$$F_H^{'} = F_H \otimes att_c(F_L \oplus F_H) \tag{7}$$

$$F_L^{'} = F_L \otimes att_s\left(F_L \oplus F_H\right) \tag{8}$$

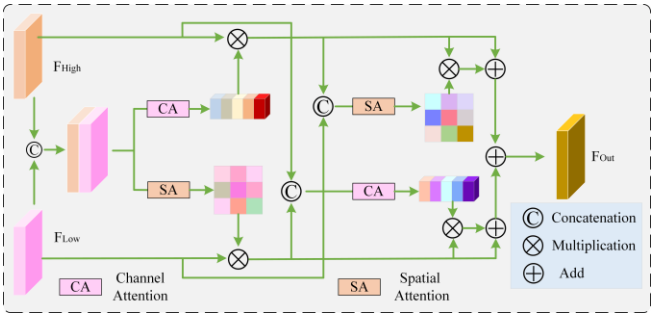

Figure 2. Attention Module Integration

Where, F_L and F_H represent low-dimensional and high-dimensional features, respectively. $F_H^{'}$ and $F_L^{'}$ represent the high and low-dimensional features obtained after processing with the channel and spatial attention modules, respectively. $\otimes$ represents the multiplication operation, $\oplus$ represents the summation operation, and att_c and att_s represent the channel attention and spatial attention, respectively.

$$att_c(F) = \sigma(f_{conv1}(G_A(F)) + f_{conv1}(G_M(F))) \quad (9)$$

$$att_s(F) = \sigma(f_{conv7}([G_A(F)); G_M(F)]) \quad (10)$$

$$F_{Out} = F_H' \otimes att_s(F_L \oplus F_H') + F_L' \otimes att_c(F_L' \oplus F_H) \quad (11)$$

Where, G_A represents global average pooling, and G_M represents global max pooling, both used to extract global information. f_{conv1} represents a 1×1 convolutional shared convolutional layer, and f_{conv7} represents a convolutional layer with a kernel size of 7×7. The combination of these two methods can effectively address the issue of weak feature representation ability. F_{Out} represents the final features obtained after the input features are processed through the channel and spatial attention modules in a cross manner.

By cross-reorganizing the channel attention module and the spatial attention module, it cleverly links information from different dimensions while differentiating the weight size based on the importance of each feature, allowing the model to better emphasize features that are useful for the task.

2.3. Multi-Sensor Data Fusion Strategy

To fully exploit the advantages of multi-sensor collaborative perception, this paper proposes a unified preprocessing and fusion scheme for heterogeneous sensor signals. Suppose the system is equipped with N acceleration sensors placed at key positions such as the bearing outer ring and horizontal/vertical directions, each recording vibration signals under the same operating condition. The raw signal of the i-th sensor is denoted as $x_i(t), i = 1, 2, ..., N$.

All sensor signals are first filtered by a band-pass filter (20–8000 Hz) to remove environmental noise and then synchronized by linear interpolation. To eliminate amplitude deviation caused by installation differences and sensitivity variation, Z-score normalization is applied:

$$\tilde{x}_i(t) = \frac{x_i(t) - \mu_i}{\sigma_i} \quad (12)$$

Where, μ_i and σ_i denote the mean and standard deviation of the i-th sensor signal, respectively. This ensures that all sensor channels share a consistent amplitude scale.

Each sensor signal is processed by the Time-Frequency Aware Convolution (TFAConv) layer to extract the corresponding time–frequency feature map $F_i \in \mathbb{R}^{C \times T}$. To achieve unified multi-source representation, the features from all sensors are concatenated along the channel dimension:

$$F_{fusion} = \text{Concat}(F_1, F_2, \ldots, F_N) \quad (13)$$

A 1×1convolution is then applied for linear projection and dimensional compression:

$$F' = \text{Conv}_{1\times1}(F_{fusion}) \quad (14)$$

Based on the fused feature F', a dual attention module—comprising channel and spatial attention—is introduced to adaptively weigh the features from different sensors. The channel attention captures the importance variation across sensors, while the spatial attention focuses on key local regions, thus enabling effective multi-source information enhancement and noise suppression.

2.4. The Fault Diagnosis Framework

The time-frequency aware convolutional layer proposed earlier is used as a preprocessing layer, combined with CNN, resulting in a new network named TFANet. By utilizing the time-frequency aware convolutional layer to extract time-frequency information related to fault factors from vibration signals, it can effectively diagnose fault types in mechanical equipment. The network architecture based on TFANet is shown in Table 1. The overall framework of the fault diagnosis method based on TFANet is illustrated in Figure 3.

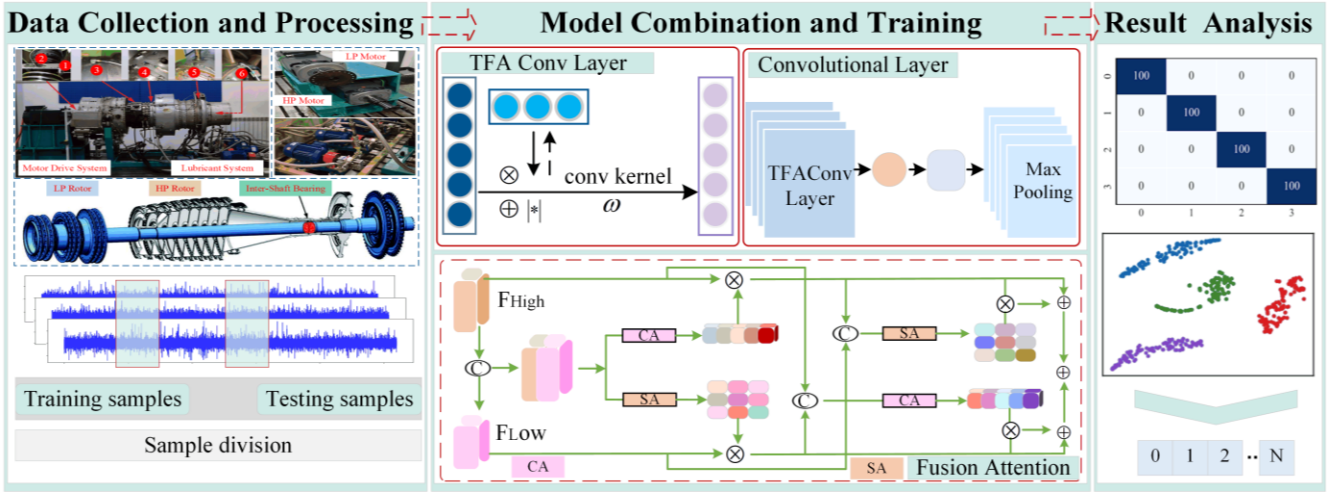

Figure 3. Fault Diagnosis Framework Diagram

First, vibration signals are collected from the bearing test rig. The time-frequency aware convolutional layer is used to capture key feature information from multi-sensor vibration signals, and the samples are labeled for training. An improved convolutional neural network is then used to extract discriminative key feature information. The established model is trained and applied to recognize test samples, ultimately outputting the fault diagnosis features.

Table1. Model Parameters

Number	Network	Kernel size	kernel	Output
	Input			3*1024
1	TFAConv	1×15/1	16	n_c*1024
2	Conv1-BN	1×3/1	32	32*1010
3	CA	1×3/1	32	32*1010
4	Conv2-BN-	1×3/1	64	64*1008
5	Maxpool	1×2/2	64	64*504
6	Conv3-BN-	1×3/1	128	128*502
7	Maxpool	1×2/2	128	128*251
8	Conv4-BN	1×3/1	256	256*249
9	SA	1×3/1	256	256*249
10	Linear(256)-ReLU-Linear(128)-ReLU-Linear(4)	——		4

3. EXPERIMENTAL VERIFICATION

In this section, in order to verify and analyze the application of the proposed TFANet method in bearing fault diagnosis, we will conduct experiments from different perspectives and report the results. The bearing datasets used in this section are vibration signals collected via accelerometers. All experimental programs were run on the following configured computer: Pytorch 1.12.0+cu113, CPU: i5-12400F, GPU: NVIDIA GeForce RTX 2060 SUPER, 16 GB RAM.

The proposed method is comprehensively compared with several mainstream fault diagnosis methods, as detailed below：

(1) Classical Convolutional Neural Network Model (Han, Shao & Jiang, 2022): Automatically extracts fault features from raw vibration signals.

(2) ResNet18 Model with Residual Connections (Wang, Chen, Wang & Shao, 2023): Achieves efficient learning and representation of deep-level features.

(3) GAAE Model with Global Perception Attention Mechanism (Yan, Shao & Ming, 2023): Achieves deep expression and compressed reconstruction of key fault features.

(4) HAGCN Model with Hierarchical Attention Mechanism and Graph Convolutional Structure (Li, Zhao & Sun, 2023): Effectively models the topological relationships of vibration signals in non-Euclidean space.

(5) DAGCN Model Combining Graph Convolutional Structure and Dual Attention Mechanism (Li, Zhao & Sun, 2021): Dynamically mines key feature information from vibration signals.

3.1. Harbin Institute of Technology Bearing Dataset.

The bearing dataset used in this study (Hou, Yi, Jin & Gui, 2023) originates from real data collected from an aviation engine. The fault diagnosis experimental platform consists of an improved aviation engine (with the rotor blades, combustion chamber, and some accessory shells removed, but retaining the dual-rotor structure of the main components), a motor drive system, a lubrication system, two eddy current sensors, and four acceleration sensors (the specific structure is shown in Figure 4). The sampling frequency for each set of signals is 25,000 Hz, with a continuous sampling time of 15 seconds.

The bearing dataset consists of four health conditions, as shown in Figure 5 and Table 2. The faults are created through wire cutting processing and include normal bearings (N), outer race faults (OF), and inner race faults (IF) with fault lengths of 0.5 and 1.0. The fault data under different health conditions are segmented using a sliding window approach. An overlapping sampling method is applied to obtain 360 samples for each category, with 70% used for the training set and 30% for the testing set.

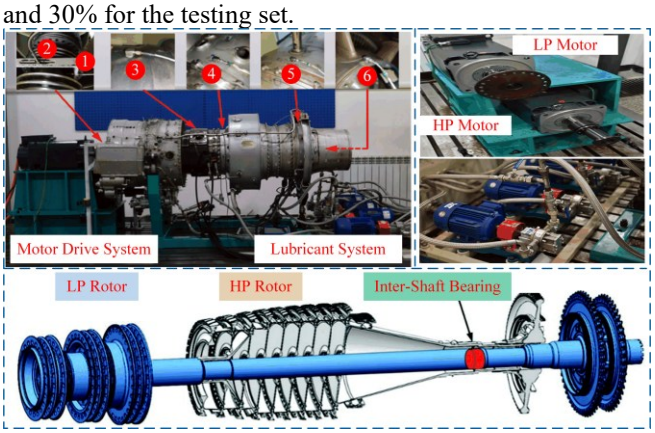

Figure 4. The Experimental Platform

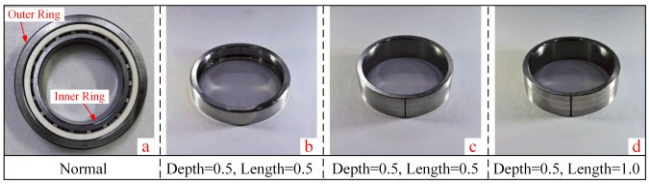

Figure 5. Bearing Health Condition

Table 2. Data Introduction.

Condition	Label	Depth of fault	Depth of fault
Normal（a）	0	—	—
OR fault（b）	1	0.5	0.5
IR fault（c）	2	0.5	0.5
IR fault（d）	3	0.5	1.0

3.2. Experimental Results and Analysis

To ensure fairness of the experiments, the hyperparameters of all comparison methods mentioned in this paper are the

same as those used in the proposed method. In each training and testing iteration, to reduce the randomness of the experiments, each method is run 10 times, and the average value is taken to make the validation more stable and convincing. The performance values after 300 training rounds are shown in the table below.

Table 3. Average Metrics.

Method	Accuracy%	variance	MAE
CNN	96.12	0.43×10^{-3}	0.132
ResNet18	96.31	0.56×10^{-3}	0.104
GAAE	97.04	0.33×10^{-3}	0.127
HAGCN	97.32	0.25×10^{-3}	0.072
DAGCN	98.54	0.18×10^{-3}	0.084
TFANet	**99.54**	$\mathbf{0.13\times10^{-3}}$	**0.051**

The confusion matrix provides an intuitive visualization of the recognition results for each fault type, quantifying the model's classification performance on each fault type. As shown in Figure 6, the comparison models achieve good diagnostic performance overall. However, in the data related to label 1 and label 2, there is noticeable feature entanglement, leading to misclassification of these two fault types in the diagnosis process.

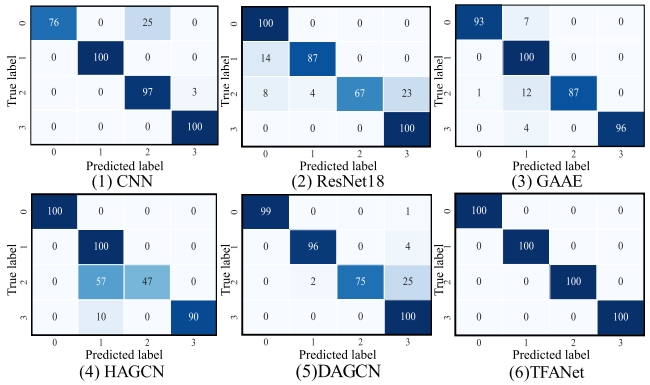

Figure 6. Confusion Matrix

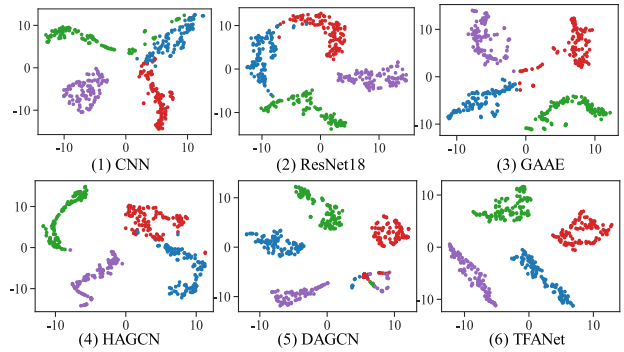

Figure7. t-SNE

The paper visualizes the feature distribution learned by different models using the t-SNE algorithm. As shown in Figure 7 (6), the proposed method significantly outperforms other methods in terms of classification performance. The distribution of the same fault type across different data domains is more compact, while the distinction between different fault categories is clearer. This indicates that the proposed model can efficiently extract key fault feature information from multi-sensor vibration signals.

To investigate the true classification performance of the model for each fault type in detail, this paper evaluates the classification performance of each model for every health condition of the bearing. As shown in Table 4.

Table 4. F1 Score of Each Label.

Label\F1	0	1	2	3
CNN	76.74	100.0	96.74	100.0
ResNet18	100.0	87.17	67.54	100.0
GAAE	93.08	100.0	87.05	95.86
HAGCN	100.0	100.0	46.79	89.97
DAGCN	99.16	96.47	75.01	100.0
TFANet	**100.0**	**100.0**	**100.0**	**100.0**

3.3. Ablation Experiment

To further validate the diagnostic performance of the proposed TFANet method, this section conducts an ablation experiment. The time-frequency aware convolutional layer is named as Module A, the feature fusion module is named as Module B, and the single-sensor vibration signal input is named as A Sensor. The combination of Modules A and B forms the TFANet method proposed in this paper. The diagnostic results of all modules are shown in Table 5.

Table 5. Evaluation Metrics of Each Module.

Method	F1	Pr(%)	Re(%)	Accuracy(%)
A	96.12	96.69	96.74	96.86
A+B	98.20	98.00	98.57	98.12
A Sensor	97.36	98.21	97.09	97.95
TFANet	**100.0**	**99.52**	**100.0**	**99.54**

Table 5 demonstrates the improvement in bearing fault diagnosis performance when integrating the time-frequency aware convolutional layer module and the feature fusion module in the proposed network architecture. The baseline model A achieves an F1 score of 96.12%. With the addition of the feature fusion module (A+B), the F1 score increases to 98.20%, indicating that this module significantly enhances feature interaction. The single-sensor input (A Sensor) also achieves some improvement, reaching an F1 score of 97.36%, though its overall performance remains slightly inferior to the multi-sensor configuration. The complete TFANet achieves the best performance across multiple metrics (F1 and Recall at 100%, Precision at 99.52%, and Accuracy at 99.54%), yielding relative improvements of 4.04%, 3.03%, 3.35%, and 2.77% over the baseline.

3.4. Sensitivity Analysis on Sensor Quantity

To evaluate the impact of sensor quantity on model performance, experiments were conducted using single-sensor, dual-sensor, and three-sensor inputs for comparison. As shown in Table 6, the diagnostic performance of the proposed model consistently improves with the increase in the number of sensors. When three sensors are used, the

model achieves the highest accuracy of 99.78% and a perfect F1-score of 100, indicating that multi-sensor fusion effectively enhances feature perception and fault discrimination capability. Further increasing the number of sensors yields only marginal improvement, suggesting that three sensors provide an optimal balance between diagnostic accuracy and system complexity. Therefore, three-sensor input is adopted as the standard configuration for TFANet in this study.

Table 6. Performance with Different Sensor Numbers.

Number	Accuracy(%)	Variance ($\times 10^{-3}$)	F1
1 Sensor	96.78	0.52	96.86
2 Sensor	98.42	0.31	98.21
3 Sensor	**99.78**	**0.13**	**100**

4. CONCLUSION

This paper proposes a deep learning model named TFANet, which designs a time-frequency aware convolutional layer as a preprocessing module and incorporates a fusion attention mechanism to enhance the feature extraction capability of the convolutional neural network. The model can effectively extract time-frequency features closely related to faults from vibration signals, enabling the modeling of long-range dependencies for key features. Experimental results show that the proposed method achieves an accuracy of 99.54% on the HIT bearing dataset, significantly outperforming existing comparison methods. Further ablation experiments validate the effectiveness of each component module of TFANet in improving fault diagnosis performance.

In summary, the TFANet model proposed in this paper demonstrates superior diagnostic performance in mechanical equipment fault diagnosis tasks, providing strong support for both theoretical research and engineering applications, and showing considerable potential for broader adoption. It should be noted that the experiments in this study are primarily based on publicly available datasets, and the model's generalization capability on additional datasets and under complex real-world operating conditions remains to be further validated. In future work, we plan to apply TFANet to multi-sensor fault diagnosis, real-time monitoring, and predictive maintenance scenarios, aiming to further enhance its practical value and contribute to the development of intelligent manufacturing.

ACKNOWLEDGEMENT

The author would like to thank Professor Hou Lei and the team of Chen Yushu from Harbin Institute of Technology for publicly providing the aero-engine bearing dataset, which offered crucial experimental support for this research.

REFERENCES

Dai, P., Liang, X., Li, J., Wu, D., & Wang, F. (2025). Modeling strategy and mechanism analysis for the dual-rotor-disc-bearing coupled system with unbalance effect in aeroengines[J]. Mechanical Systems and Signal Processing, 2025, 224: 112086.

Kim, S., & Lee, S. (2025). Fault-relevance-based, multi-sensor information integration framework for fault diagnosis of rotating machineries[J]. Mechanical Systems and Signal Processing, 2025, 232: 112742.

Li, X., Chen, H., & Li, S. (2025). Multi-kernel weighted joint domain adaptation network for cross-condition fault diagnosis of rolling bearings[J]. Reliability Engineering & System Safety, 2025: 111109.

Liu, Y., Chen, Y., Li, X., Zhou, X., & Wu, D. (2025). MPNet: A lightweight fault diagnosis network for rotating machinery[J]. Measurement, 2025, 239: 115498.

Xiao, X., Li, C., & He, H. (2025). Rotating machinery fault diagnosis method based on multi-level fusion framework of multi-sensor information[J]. Information Fusion, 2025, 113: 102621.

Xu, Z., Chen, X., & Xu, J. (2025). Multi-modal multi-sensor feature fusion spiking neural network algorithm for early bearing weak fault diagnosis[J]. Engineering Applications of Artificial Intelligence, 2025, 141: 109845.

Yang, Z., Li, G., Xue, G., & He, B. (2025). A novel multi-sensor local and global feature fusion architecture based on multi-sensor sparse Transformer for intelligent fault diagnosis[J]. Mechanical Systems and Signal Processing, 2025, 224: 112188.

Han, S., Shao, D., & Jiang, H. (2022). Intelligent fault diagnosis of aero-engine high-speed bearings using enhanced CNN[J]. Acta Aeronautica et Astronautica Sinica, 2022, 43(9): 158-171.

Wang, P., Chen, J., Wang, Z., & Shao, W. (2023). Fault diagnosis for spent fuel shearing machines based on Bayesian optimization and CBAM-ResNet[J]. Measurement Science and Technology, 2023, 35(2): 025901.

Yan, S., Shao, H., & Min, Z. (2023). FGDAE: A new machinery anomaly detection method towards complex operating conditions[J]. Reliability Engineering & System Safety, 2023, 236: 109319.

Li, T., Zhao, Z., & Sun, C. (2023). Hierarchical attention graph convolutional network to fuse multi-sensor signals for remaining useful life prediction[J]. Reliability Engineering & System Safety, 2021, 215: 107878.

Li, T., Zhao, Z., & Sun, C. (2021). Domain adversarial graph convolutional network for fault diagnosis under variable working conditions[J]. IEEE Transactions on Instrumentation and Measurement, 2021, 70: 1-10.

Hou, L., Yi, H., Jin, Y., & Gui, M. (2023). Inter-shaft bearing fault diagnosis based on aero-engine system: a benchmarking dataset study[J]. Journal of Dynamics, Monitoring and Diagnostics, 2023: 228-242.